Spatial and temporal trends for water-flow velocity and bed-material sediment transport in the lower Mississippi River

Jeffrey A. Nittrouer[1,†], John Shaw[1], Michael P. Lamb[2], and David Mohrig[1]
[1]*Department of Geological Sciences, University of Texas, 1 University Station C9000, Austin, Texas 78712, USA*
[2]*Division of Geological and Planetary Sciences, California Institute of Technology, MC 170-25, 1200 E. California Boulevard, Pasadena, California 91125, USA*

ABSTRACT

Where rivers near the coastline, the receiving basin begins to influence flow, and gradually varied, nonuniform flow conditions arise. The section of the river affected by nonuniform flow is typically referred to as the backwater segment, and for large lowland rivers, this portion of the river can extend many hundreds of kilometers above the outlet. River morphology and kinematics vary in the backwater segment; however, these channel properties have not been explicitly related to properties of the flow and sediment-transport fields. This study examines the influence of spatially and temporally varying flow velocity and sediment transport on channel properties for the lower 800 km of the Mississippi River, a section of the river that includes the backwater segment. Survey transects (n = 2650) were used to constrain the cross-sectional area of water flow every ~312 m along the Mississippi River channel for eight successive intervals of water discharge. Assuming conservation of water discharge, the local flow velocity was calculated at each transect by dividing water discharge by the local measurement of cross-sectional flow area. Calculated flow velocity was converted to total bed stress using a dimensionless friction coefficient that was determined by optimizing the match between a predicted and a measured water-surface profile. Estimates for the skin-friction component of the total bed stress were produced from the values for total shear stress using a form-drag correction. These skin-friction bed-stress values were then used to model bed-material transport. Results demonstrate that in the lower Mississippi River, cross-sectional flow area increases downstream during low- and moderate-water discharge. This generates a decrease in calculated water-flow velocity and bed-material transport. During high-water discharge, the trend is reversed: Cross-sectional flow area decreases downstream, producing an increase in calculated water-flow velocity and bed-material transport. An important contribution of this work is the identification of a downstream reversal in the trend for channel cross-sectional area due to variable water discharge. By accounting for the spatial divergences in sediment transport predicted over an average annual hydrograph, we demonstrate the tendency for channel-bed aggradation in much of the backwater reach of the Mississippi River (150–600 km above the outlet); however, a region of channel-bed erosion is calculated for the final 150 km. These results help to explain the spatial variability of channel morphology and kinematics for the lower Mississippi River, and they can be extended to other lowland river systems near the coastline.

INTRODUCTION

Backwater Hydrodynamics and Channel Character

Where a river approaches its outlet, river flow tends to decelerate downstream due to channel deepening, and the segment of river where this response occurs defines the backwater segment (Chow, 1959). The length of a backwater segment (L_b) is evaluated by the momentum equation for open-channel flow, and it is scaled by characteristic flow depth (H) and water-surface slope (S): $L_b = HS^{-1}$ (Paola and Mohrig, 1996). Particularly in low-sloping rivers ($S \leq 10^{-5}$), such as the Mississippi River (H = 10–30 m), the backwater reach can extend hundreds of kilometers upstream of the outlet. Dynamic flow conditions in this portion of the river play a critical yet underevaluated role in physically shaping rivers in coastal zones by altering the spatial and temporal conditions of sediment transport (Nittrouer et al., 2011a).

Within the source-to-sink framework, the backwater segments of rivers have been neglected from detailed studies, despite the fact that hydrodynamic processes in these reaches modulate the transfer of sediment from Earth's land surface to marine settings (Nittrouer et al., 2011a). In this study, we calculate spatial and temporal changes in flow velocity and the associated divergences in sediment transport for a large, deep river near the coastline. In particular, this study demonstrates that the transition from reach-averaged steady and uniform flow (normal flow) to gradually varying backwater flow alters the timing and magnitude of bed-material transport within the river channel, and its delivery to the river outlet.

Changes in channel planform and kinematics, and bed-material sediment composition are noted to arise near the outlets of alluvial river systems (Lane, 1957). For example, Ikeda (1989) described adjustments in bed-material composition, channel migration, and incision versus aggradation in the Teshio River (Japan) as it approaches its Sea of Japan outlet. Near the coastline, the Teshio River is characterized by channel bends that are relatively fixed (limited lateral migration) and incised into previous floodplain deposits. Progressing upstream, bed-material sediment coarsens and sinuosity and lateral migration increase. Still farther upstream, in the vicinity of the backwater transition (L_b = 20 km: H = 6 m, S = 3×10^{-4}), bed material continues to coarsen, and channel cutoffs preserved as oxbow lakes become more frequent. Here, the channel-bed elevation aggrades relative to the surrounding floodplain, facilitating avulsions. These observations depict a lowland fluvial system with dynamic channel properties that coincide with the backwater reach, where the system is influenced by nonuniform flow conditions. This

†Current address and e-mail: Department of Geology, University of Illinois at Urbana-Champaign, 253 Natural History Building, Urbana, Illinois 61801, USA; jeffnitt@illinois.edu

GSA Bulletin; March/April 2012; v. 124; no. 3/4; p. 400–414; doi: 10.1130/B30497.1; 13 figures; 2 tables.

study explores the way in which water flow in the backwater segment of a river affects sediment transport, thereby facilitating changes in channel properties such as distribution and character of alluvial sands and diminished rates of lateral mobility, similar to those qualitatively observed for the Teshio River.

Backwater Influence on Bed-Material Transport in the Mississippi River

Extensive sampling of the channel bottom in the lower Mississippi River reveals that bed materials consist of all grains greater than 63 µm (Allison and Meselhe, 2010). This component of sediment translates as a part of both suspended-load and bed-load transport (Nittrouer et al., 2008, 2011b). Hydrodynamic flow conditions in the backwater reach of the Mississippi River have an important role for regulating the downstream transport of bed-material sediment. Measurements collected 40 km from the river outlet document a hundredfold increase in bed-material flux for a fourfold increase in water discharge (low- to high-water discharge; Nittrouer et al., 2011a). Coincident with this increase in sediment flux, there is a nearly tenfold increase in the skin-friction component of the boundary shear stress. Such significant changes in stress and sand flux are not possible where reach-average normal-flow conditions persist in the Mississippi River, above roughly 650 km upstream of the river outlet (Fig. 1; Nittrouer et al., 2011a).

Backwater hydrodynamics affect bed-material movement in the Mississippi River by reducing skin-friction stress to near the critical threshold for sand mobility during low- and moderate-water discharge, thereby shutting down suspended bed-material transport and resulting in only minimal bed-load flux (Nittrouer et al., 2011a). In the normal-flow segment upstream,

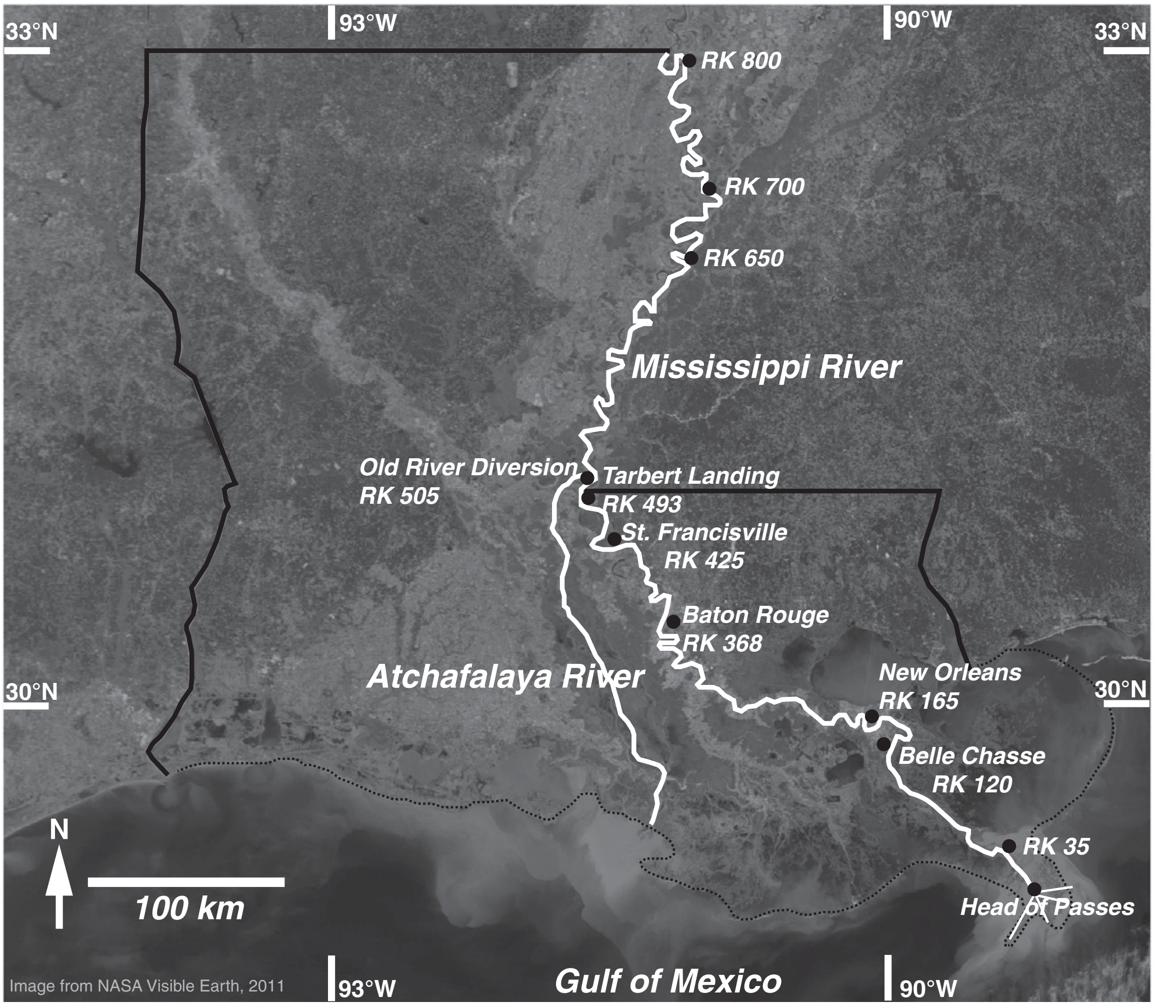

Figure 1. The lower 800 river kilometers of the Mississippi River; the state of Louisiana is outlined. Cross-channel transect data collected by the USACE, 1974–1975 (Harmar, 2004) were used to construct the cross-sectional area of the lower Mississippi River from RK 800 (RK—river kilometers above the outlet) to Head of Passes (HOP; the outlet of the Mississippi River). In total, 2650 transects were used, spaced downstream by an average distance of 312 m. Locations labeled are referenced in this study: backwater flow begins near RK 650 (coincidently where the channel-bed elevation begins to fall below sea level); Old River Diversion is where the Atchafalaya River exits the main stem Mississippi River (RK 505). Velocity data used in this study were collected by the USACE at Tarbert Landing (RK 493), Baton Rouge (RK 368), and New Orleans (RK 165). Suspended-sediment data referenced in this study were collected by the U.S. Geological Survey (USGS) at St. Francisville (RK 425) and Belle Chasse (RK 120).

reach-average flow velocities are uniform, and stress is sufficient for both suspended-load and bed-load transport of bed materials during low- and moderate-water discharge. The reduction in stress in the backwater reach reduces bed-material mobility, leading to a downstream decrease in sediment transport that is hypothesized to produce deposition and storage of bed materials in the river channel (Nittrouer et al., 2011a). Because the Gulf of Mexico is a mircrotidal environment (<30 cm), tides do not have a significant influence on sediment transport dynamics in the lower few hundred kilometers of the river (Nittrouer et al., 2008).

Unknown factors include the location, volume, and duration of bed-material deposition in the backwater reach of the Mississippi River. For example, how do the significantly enhanced skin-friction stresses measured in the backwater segment from low- to high-water discharge affect deposition and storage of bed materials? These questions can be addressed by evaluating temporal and spatial changes in flow velocity and sediment transport through the backwater segment of the Mississippi River. In this study, we calculated flow velocity for a variety of water-discharge conditions by compiling data for local bed topography and stage height in order to estimate the cross-sectional area of flow, and dividing this value into the respective water discharge. Local flow velocity was converted to skin-friction shear stress and used to estimate spatial and temporal divergence in the bed-material flux based on a bed-load transport model. The analysis concludes by describing the ways in which the dynamics of bed-material transport facilitate storage of sediment in the channel, and affect measured channel properties of the Mississippi River, including distribution and character of alluvial sand cover and rates of lateral mobility.

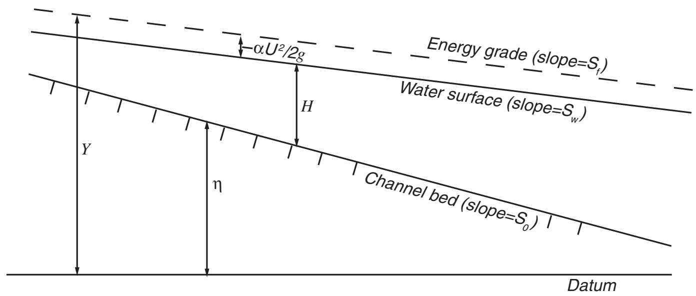

Figure 2. Schematic illustration for gradually varying open-channel flow defining the backwater condition (after Chaudhry, 2008). Variables in figure: S_0 is the channel-bed slope, S_w is the water-surface slope, S_f is the energy-grade slope, Y is the total energy grade, η is the channel-bed elevation, H is the flow depth, U is flow velocity (m s^{-1}), α = 1.15–1.5 (an energy coefficient), and g is gravitational acceleration.

Backwater Flow Description

Where normal-flow conditions preside in a river, the channel-bed slope (S_0), water-surface slope (S_w), and energy-grade slope (S_f) are uniform. However, as a river approaches its outlet, the channel-bed elevation drops below sea level, and bed and water slope deviate. The river's water-surface profile asymptotically approaches the mean water elevation of the receiving basin. Flow begins to lose gravitational potential and decelerate due to a gradual downstream deepening. This effect of gradually varied flow reduces the total energy grade (Y), which is shown in Figure 2 and is expressed as

$$Y = \eta + H + \frac{\alpha U^2}{2g}, \tag{1}$$

where η is the channel-bed elevation, H is the flow depth, U is flow velocity (m s^{-1}), α = 1.15–1.5 (an energy coefficient), and g is gravitational acceleration (e.g., Chaudhry, 2008). To determine the energy-grade slope associated with backwater flow, Equation 1 is differentiated with respect to x:

$$\frac{dY}{dx} = \frac{d\eta}{dx} + \frac{dH}{dx} + \frac{\alpha Q_w^2}{2g}\frac{d}{dx}\frac{1}{\left(A^2\right)}, \tag{2}$$

where $U = Q_w A^{-1}$ (Q_w = constant water discharge, m^3 s^{-1}, and A = cross-sectional flow area, m^2), and

$$\frac{d}{dx}\frac{1}{A^2} = \frac{d}{dA}\frac{1}{A^2}\left[\frac{dA}{dH}\frac{dH}{dx}\right] = \frac{-2B}{A^3}\frac{dH}{dx}, \tag{3}$$

where B is width, and is substituted for dA/dh assuming a prismatic channel. Making the substitutions $dY/dx = -S_f$ and $d\eta/dx = -S_0$ yields

$$-S_f = -S_0 + \frac{dH}{dx}\left(1 - \frac{\alpha Q_w^2 B}{gA^3}\right). \tag{4}$$

The last term in Equation 4 is equal to (1 – Fr^2), where the Froude number is Fr = $U(gH)^{-0.5}$. For this special case, downstream change in flow depth (dH/dx) is equal to

$$\frac{dH}{dx} = \frac{S_0 - S_f}{1 - \mathrm{Fr}^2}. \tag{5}$$

Alternatively, using the equation for conservation of momentum for open-channel flow, a substitution for S_f can be made:

$$S_f = \frac{\tau_b}{\rho g H}, \tag{6}$$

where $\tau_b = \rho C_f U^2$ is the total boundary shear stress, C_f is the dimensionless bed resistance coefficient, and ρ is water density (e.g., Chow, 1959; Parker, 2004). Therefore, Equation 5 is rearranged to

$$\frac{dH}{dx} = \frac{S_0 - C_f \mathrm{Fr}^2}{1 - \mathrm{Fr}^2}. \tag{7}$$

For the lower Mississippi River, the variables water discharge (Q_w), channel-bed elevation (η) and slope (S_0), and water-surface elevation and slope (S_w) are known. Water-surface slope departs from the channel-bed slope at ~RK 650 (where RK refers to river kilometers above the outlet at Head of Passes; Figs. 1 and 3), a position in the river where the thalweg and 40th percentile channel-bed elevation (η_{40}) drop below mean sea level (~RK 700 and ~RK 600, respectively; Fig. 3). Near this transition, measured flow velocity decreases downstream during low- and moderate-water discharge (Nittrouer et al., 2011a), marking a backwater condition in the Mississippi River where the system approaches its coastline and outlet at the Gulf of Mexico.

Equation 7 has been applied in previous studies that seek to evaluate backwater hydrodynamics and effects on sediment transport associated with rivers entering man-made reservoirs (e.g., Snyder et al., 2006), or to evaluate the dynamics of sediment routed through lowland rivers to a neighboring receiving basin (Parker et al., 2008). In this study, we examine the morphodynamic interactions on yearly (flood interval) time scales, in order to assess the way in which sediment transport in a fluvial system near its marine outlet is affected by nonuniform flow conditions, and in turn, the way in which variability in sediment transport affects river-channel morphology.

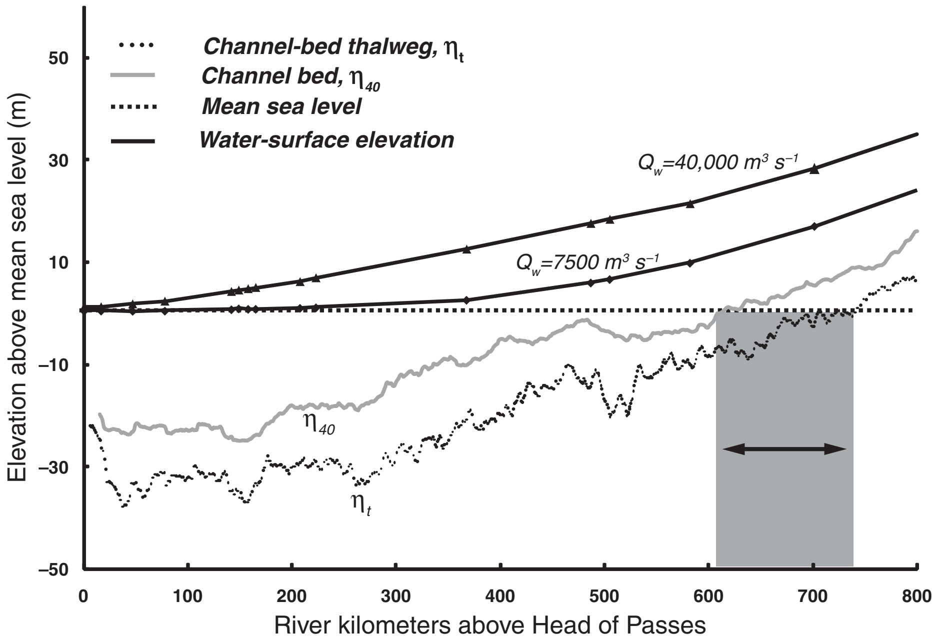

Figure 3. Profile of the channel-bed and water-surface elevation for two water-discharge conditions (Q_w = 7500 and 40,000 m^3 s^{-1}). The triangles (high flow) and diamonds (low flow) are the gauging station data (Table 1); stage data were fit with a six-order polynomial regression function to generate a smoothed water-surface profile. The thalweg profile (η_t) was constructed using the USACE cross-channel-transect survey data, collected in 1974–1975 (Harmar, 2004), for the lower 800 km of the Mississippi River (n = 2650 transects, spaced ~312 m apart). The profile was determined by finding the maximum depth of each cross-channel transect and then applying a downstream box-car averaging function to the data (30 km window). The channel-bed elevation profile (η_{40}) was determined by finding the 40th percentile elevation for each transect, beginning from the channel bed, and then applying a downstream box-car averaging function to the data (30 km window). The gray box highlights the location between RK 600 and 750 near the location where η_{40} and η_t intercept the elevation of mean sea level.

TABLE 1. NAME OF STAGE GAUGE SITE AND LOCATION ON THE MISSISSIPPI RIVER

Stage site name (USACE data)	River kilometer (RK) above Head of Passes (HOP)
Head of Passes	0
Venice	17.2
Empire	47.5
La Hache	78.4
Algeirs	142.2
IHNC	149.2
Harvey Lock	158.3
Carrolton	165.5
Bonnet Carre	208
Baton Rouse	367.7
Red River	486.9
Knox Landing	505.1
Natchez	582
Vicksburg	701.5
Greenville	855.4
Arkansas City	892.1
Helena	1067.4

Note: Stage data from these sites were used to determine water-surface-elevation profile for the discharge ranges modeled in this study. Data are available from the U.S. Army Corps of Engineers (USACE). IHNC—Inner Harbor Navigation Canal.

METHODS

Determining Cross-Sectional Area of Flow for the Lower Mississippi River

This study uses channel survey data collected by the U.S. Army Corps of Engineers (USACE; data collected 1974–1975; found in: Harmar, 2004, appendix) and measures cross-sectional area of flow for a range of water-discharge conditions across the normal-flow to backwater transition in the Mississippi River. The survey data consist of channel-bottom transects positioned perpendicular to the local downstream channel orientation; elevation measurements along each transect were collected every ~30–50 m, and they record the local levee tops on both bank lines. All survey elevation data are referenced to NGVD 1929 and have been converted to meters above mean sea level. Each transect is spaced by an average downstream distance of 312 m; the midpoint is referenced to distance above the river outlet at Head of Passes (HOP; Fig. 1). The USACE channel survey data extend from HOP to Cairo, Illinois (*RK* 1700); however, for this study, only the lower 800 km section is considered (n = 2560 transects); this data range covers the channel from the normal-flow segment through the backwater reach (Fig. 1).

Cross-sectional area of water flow was measured at each transect by coupling local water-surface elevation and transect profiles. Stage-elevation data were collected at 18 gauge sites in the lower 1100 km of the Mississippi River (Table 1) over the time period 1977–1985 (www.rivergauges.com). Daily stage elevation recorded at each gauge site was tied to the daily water-discharge data collected at Tarbert Landing (n = 3287). Daily stage elevation data were binned and averaged at each gauge, using eight water-discharge bins, 5000 m^3 s^{-1} in size (i.e., <5000, 5000–10,000,…, 30,000–35,000, and the last bin, >35,000 m^3 s^{-1}). All stage elevations at each gauge for each discharge bin were averaged; for each discharge bin, the average water-surface elevations for the 18 gauges were plotted against distance above the outlet and fit with a six-order polynomial regression function to generate a smoothed water-surface profile for each discharge bin (regression function that minimized residuals while providing a smooth fit). This method of averaging elevation data ensures that the elevation profiles developed for each discharge bin are not biased by individual flood waves; importantly, the stage variability at each gauge over the water-discharge range of the bins does not significantly alter the water-surface-elevation profile generated by the regression function. Using the formula from the regression function, water-surface elevation at each transect was calculated for each discharge bin (e.g., the input is channel distance from the outlet for each transect, and output is water-surface elevation).

Cross-sectional area for the water flow ($A_{transect}$) was calculated for each transect by determining the area between the water-surface elevation and the transect profile, using a linear midpoint finite-difference scheme (Fig. 4). Channel width ($w_{transect}$) was also measured for each transect (Fig. 4). This technique was repeated for each discharge bin, using the respective water-surface elevation predicted for each transect. Flow depth was determined by finding the distance between the water-surface elevation and a selected channel-bed elevation from each transect. For example, H_{wd40} is the water depth calculated by differencing the water-surface elevation from the 40th-percentile depth from the distribution of all wetted elevations for a transect, beginning from the channel bed (i.e., H_{wd40} is slightly deeper than the median flow depth, H_{wd50}).

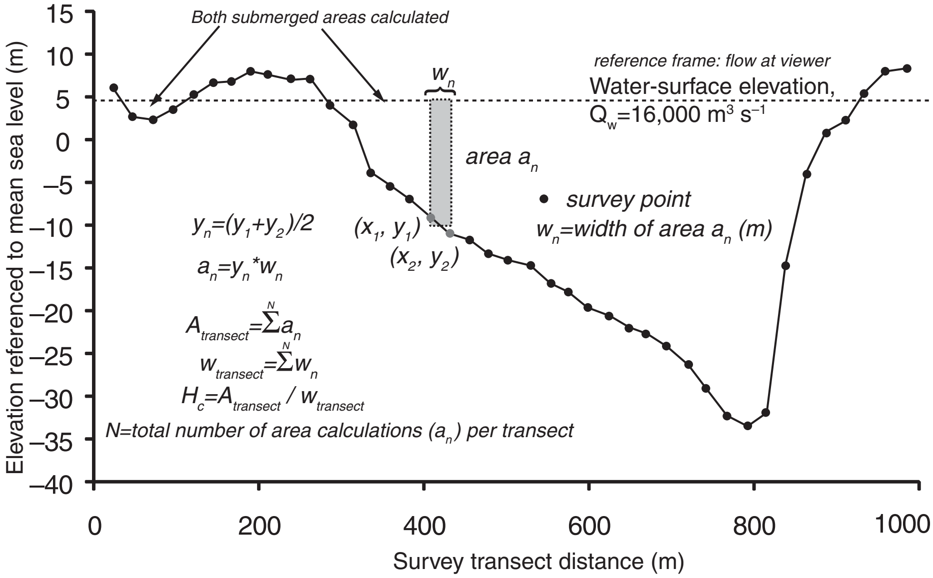

Figure 4. Cross-sectional profile from a USACE transect, collected at RK 348. The diagram indicates how cross-sectional area of water flow was calculated for each transect. A water-surface elevation for a given water discharge was calculated at each transect using a regression function fit to stage data (see text for details). This water-surface elevation was used to determine the cross-sectional area of the channel. Area between all neighboring survey points (a_n) below the water-surface elevation was calculated as the product of the across-channel distance between two neighboring points (w_n), and the average water depth between the points ($y_n = [y_1 + y_2]/2$). Total cross-sectional area for the wetted transect ($A_{transect}$) was taken as the sum of cross-sectional areas determined for all neighboring survey points ($\sum^N w_n$, where N is the total number of neighboring areas calculated per transect—equal to the number of survey points below the water-surface elevation minus one); transect width ($w_{transect}$) was taken as the sum of the widths for neighboring survey points ($\sum w_n$). Characteristic transect depth (H_c) was calculated as $A_{transect}/w_{transect}$. For some transects, islands or other topographic highs rise above the water-surface elevation of the river and split the flow. In these circumstances, area of the flow was determined as the sum of both separated areas.

Calculating Flow Velocity for the Lower Mississippi River

Water-flow velocity was calculated at each transect ($U_{transect}$) by dividing the average water discharge (Q_w) for each bin by the measured transect cross-sectional area (i.e., $Q_w/A_{transect}$). This method assumes that water discharge is conserved in the Mississippi River. Relative to the measured water discharge in the main stem Mississippi River, addition or loss of water is minimal in the lower 800 river kilometers, with the exception of Old River diversion (RK 505, Fig. 1). Here, approximately 30% of the main stem Mississippi River water discharge is diverted down the Atchafalaya Basin (value consistent with USACE operations, which regulate flow through the diversion). A spatial modification was made to account for this loss of water by adding 30% of the Tarbert Landing discharge to the Q_w above RK 505. The calculation for $U_{transect}$ was stopped at RK 35, because at this location, water begins to leave the main channel, marking the upstream location of the modern subaqueous delta complex.

Predicting Sediment Transport and Channel-Bed Elevation Changes in the Lower Mississippi River

In order to predict bed-load sediment transport in the lower Mississippi River, velocity values were converted to shear-velocity values (u_{*total}) using the relationship

$$u_{*total} = \sqrt{C_f U^2_{transect}} \tag{8}$$

(e.g., Parker, 2004; Chaudhry, 2008). To determine an appropriate value of C_f, spatial variation of water-surface elevation was modeled for each of the eight water-discharge ranges, using Equation 7. This one-dimensional backwater model uses a water discharge, per-unit-width, calculated by dividing the average water discharge, Q_w, for each discharge bin, by average channel width determined for the lower 800 km of the Mississippi River; per-unit-width water discharge is divided by local flow depth to produce $U_{transect}$, which is used to calculate the Fr term in Equation 7. Channel-bed slope (S_0) is required for the model, and this was determined from a channel-bed elevation profile. Channel-bed elevation was determined by choosing a depth percentile and finding the corresponding elevation at each transect from the distribution of wetted elevations (e.g., η_{50} is the median transect elevation). The channel-bed elevation profile was then constructed by plotting all transect-elevation values from HOP to RK 800, and applying a downstream box-car averaging function (30 km window) to the transect-elevation values in order to smooth the profile. The C_f value was then adjusted to optimize the fit between the predicted water-surface elevation (Eq. 7) and the measured water-surface profile.

Estimates of C_f proved to be sensitive to the chosen depth percentile used to construct the channel-bed elevation profile, so that choosing a deeper flow reduced the value of C_f. For example, given high-water discharge (Q_w = 38,400 m^3 s^{-1}), bed topographies of η_{50}, η_{40}, and η_{30} (i.e., progressively deepening flow) generate C_f values of 0.03, 0.045, and 0.05, respectively (Table 2). In order to evaluate the channel-bed profile that provided the optimal C_f value, we compared predicted u_{*total} (via Eq. 8) with measured u_{*total} values, collected from field surveys at three locations in the Mississippi River (RK 165, 100, and 40; Nittrouer et al., 2011a). The η value found to provide the C_f that gives the best u_{*total} match, consistent for all water-discharge conditions, is η_{40}, or an elevation profile that is slightly deeper than the median channel-bed-elevation profile. Therefore, water-surface elevation modeling to evaluate C_f for each discharge range used the η_{40} bed profile (Fig. 5). We found that a single C_f value is adequate to give a spatially consistent fit of the model to measured profiles; the slight divergence between the measured and modeled profile between RK 400 and 600 is likely associated with the relative increases in bed elevation in this region (Fig. 5; e.g., Harmar and Clifford, 2007).

Bed-roughness measurements were used to estimate the component of skin-friction shear velocity (u_{*sf}) from the total shear velocity (u_{*total}). The method uses a ratio u_{*sf}:u_{*total}, determined from form-drag measurements made at RK 35–45, and RK 160–165, based on previous studies in the lower Mississippi River (Nittrouer et al., 2011a), which use the methods of Nelson

TABLE 2. DIMENSIONLESS FRICTION COEFFICIENT VALUES AND WATER DISCHARGE FOR THE LOWER MISSISSIPPI RIVER

Q_w ($m^3\ s^{-1}$)	Modeled C_f using η_{40}		
5000	0.0075		
7500	0.0085		
12,500	0.007		
17,500	0.006		
22,500	0.006		
27,500	0.006		
32,500	0.005		
40,000	0.004		
		C_f	
Q_w ($m^3\ s^{-1}$)	η_{50}	η_{40}	η_{30}
11,750	0.0055	0.007	0.008
38,400	0.003	0.0045	0.005

Note: The dimensionless friction coefficient (C_f) values were evaluated to optimize the fit between the measured water-surface elevation and the water-surface elevation predicted by the backwater model (Eq. 7), calculated for the lower 800 km of the Mississippi River (e.g., Fig. 5).

The backwater model requires the input of a channel-bed profile; this was generated using USACE cross-channel transects (for the lower 800 km, n = 2650; Harmar, 2004), choosing a depth percentile, and finding the corresponding elevation at each transect from the distribution of wetted elevations beginning from the thalweg (for example, η_{40} is slightly deeper than the median channel depth, η_{50}). A box-car averaging technique (30 km window) was then applied to smooth the transect data (see Fig. 3 for smoothed profile). In order to evaluate the channel-bed profile that provided the optimal C_f value, predicted u_{*total} values (via Eq. 8) were compared with measured u_{*total} values, collected from field surveys at three locations in the lowermost Mississippi River (RK 165, 100, and 40; Nittrouer et al., 2011a). The η found to provide the C_f with the best u_{*total} match, consistent for all water-discharge conditions, is η_{40}. Bottom section of table shows water-discharge conditions when field surveys were conducted, and C_f values associated with using different channel-bed elevation profiles (i.e., η_{50} = median channel-bed elevation). These values establish a weak dependence of drag coefficient with discharge and representative depth.

and Smith (1989a). At low flow (<17,500 $m^3\ s^{-1}$), it was determined that $u_{*sf} = 0.60 \times u_{*total}$, and at high flow (22,500–40,000 $m^3\ s^{-1}$), it was determined that $u_{*sf} = 0.70 \times u_{*total}$. Any error incurred using these ratios is expected to be small, because the u_{*sf}:u_{*total} ratio does not change substantially from low- to high-water discharge. Additionally, we assume that bed-form morphology is similar farther upstream for comparable discharges, and because much of the channel roughness is accounted for in the bed forms, we assume that changes in u_{*sf}:u_{*total} due to adjustments in channel planform or changes in size of bedforms are relatively small. Skin-friction shear velocity values were then converted to skin-friction shear stress ($\tau_{sf} = u_{*sf}^2\rho$).

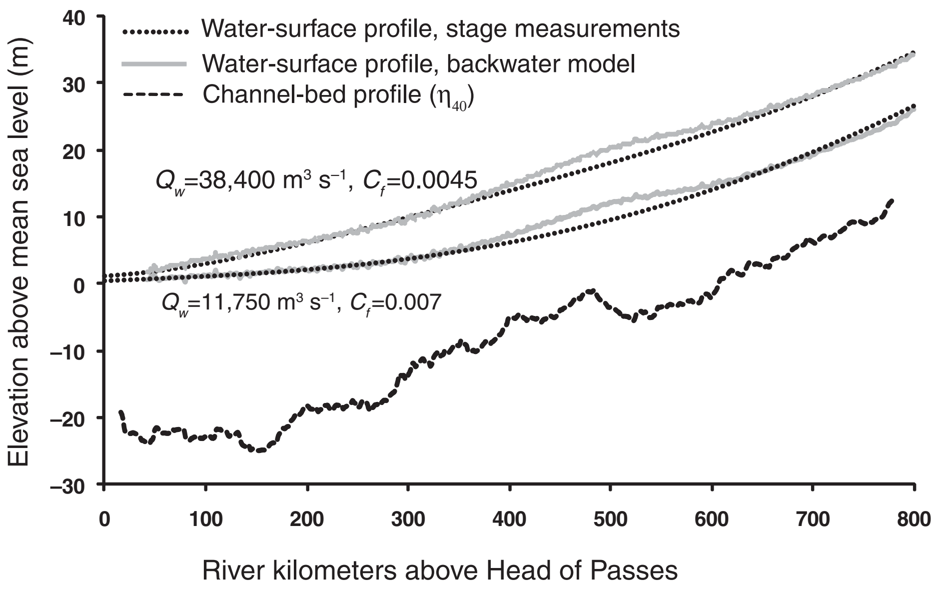

Figure 5. Water-surface profiles measured for water discharges Q_w = 11,750 and 38,400 $m^3\ s^{-1}$, fit with water-surface profiles predicted using the backwater equation (Eq. 7). The dimensionless coefficient of friction (C_f) was adjusted to optimize the fit of the model to the data. A single C_f value is adequate to provide a spatially consistent fit of the model to the measured profiles, despite the divergences near RK 400–600.

In this study, we used the bed-load transport formulation of Ashida and Michiue (1972), because previous analyses comparing bed-load transport models to field measurements in the Mississippi River have shown that this particular formula is not biased toward low or high estimates of bed-load transport rates (Nittrouer et al., 2011a). The formula relates dimensionless skin-friction stress, τ_{sf}^* ($\tau_{sf}^* = \tau_{sf}/[\rho_s - \rho]gD_{50}$, where ρ_s is density of sediment [2650 kg m^{-3}], and D_{50} is the median grain diameter), to the dimensionless critical shear stress, τ_{cr}^* ($\tau_{cr}^* = \tau_{cr}/[\rho_s - \rho]gD_{50}$, where τ_{cr} is the Shields [1936] critical shear stress for the grain diameter modeled), and provides a dimensionless bed-load transport (q_b^*):

$$q_b^* = 17\left(\tau_{sf}^* - \tau_{cr}^*\right)\left(\sqrt{\tau_{cr}^*}\right). \qquad (9)$$

Critical shear stress (τ_{cr}) was determined based on channel-bed grain-size data measured over the lower 900 river kilometers by the USACE (USACE Paper 17, 1935). Median sand grain diameter was plotted against distance above HOP (n = 183), and an exponential regression function was fit to the data; the formula for this regression function was used to determine grain size at the location of each channel transect (Fig. 6). Dimensionless bed-load transport rates were determined by combining the predicted τ_{sf}^* and τ_{cr}^* based on the calculated local transect velocity and grain size. These values were then made dimensional ($m^2\ s^{-1}$) using

$$q_s = q_s^*\left[\left(\frac{\rho_s - \rho}{\rho}\right)gD_{50}^3\right]^{0.5}. \qquad (10)$$

Two specific water-discharge conditions were considered: 11,750 and 38,400 $m^3\ s^{-1}$, because sediment-transport and shear-velocity measurements have been made at RK 35–45 for these water discharges (Nittrouer et al., 2011a), and can therefore be used for comparison to predictions in this study.

The Exner equation was used to evaluate the tendency for the channel bed of the Mississippi River to aggrade or erode based on the predictions for bed-load sediment transport. The simplified one-dimensional Exner equation (e.g., Paola and Voller, 2005) conserves mass to calculate the change in bed elevation ($\partial\eta$) based on change in bed-load sediment transport (∂q_s) over a downstream distance (∂x):

$$\left(1 - \lambda_p\right)\frac{\partial \eta}{\partial t} = -\frac{\partial q_s}{\partial x}, \qquad (11)$$

where λ_p is equal to the bed porosity (assumed to be 0.35), and ∂t is the change in time over the measurement. This simplified Exner formula-

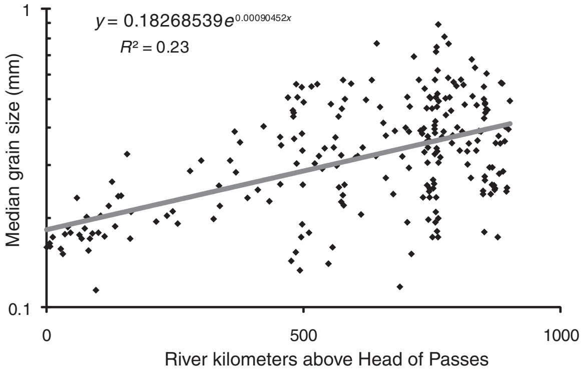

Figure 6. Channel-bed grain-size data, median diameter, collected in the lower 900 km of the Mississippi River (USACE Report 17, 1935). The exponential regression function fit to the data was used to find an appropriate grain size for evaluating critical shear stress (τ_{cr}) used in the bed-load sediment-transport modeling.

tion neglects the term for the rate of change in sediment concentration in the flow per bed area ($\partial V_s/\partial t$), which is typically added to the right side of Equation 11, by assuming that these values are much smaller than spatial changes in sediment flux (i.e., $\partial q_s/\partial x >> \partial V_s/\partial t$). To create an appropriate model for bed-elevation change in the lower Mississippi River, the proportion of time over which the modeled discharge ranges occur was determined (p_d) by using daily discharge measurements over the period 1961–2008. The model time period was set at 1 yr, and the proportion of time for each discharge range (p_d) was multiplied by the number of seconds in one year to assess ∂t. Change in sediment transport (∂q_s) was determined as the difference in predicted sediment transport between neighboring transects, and the change in downstream distance (∂x) was defined as the distance between neighboring transects. Change in channel-bed elevation was calculated for each discharge range and summed over the eight discharge ranges modeled at each transect location, to evaluate the elevation change over an average annual hydrograph.

RESULTS

Changes in Cross-Sectional Area of Flow in the Lower Mississippi River

Cross-sectional areas for each water-discharge range were plotted against distance above the outlet, and were fit with a sixth-order polynomial regression function. For example, two discharge conditions are analyzed in Figure 7A: a low flow measuring 10,000–15,000 $m^3 s^{-1}$, and a high flow measuring >35,000 $m^3 s^{-1}$. Figure 7B plots the ratio of the cross-sectional areas for each transect, and Figures 8A and 8B plot H_{wd40} and $w_{transect}$, respectively, for these discharge ranges.

There are notable spatial trends in cross-sectional area of the lower Mississippi River that vary as a function of the water discharge (Fig. 7A). During low-water discharge, cross-sectional area increases downstream, from a value near 10,000 m^2 above RK 400, to a value of 16,500 m^2 at HOP. However, during high-water discharge, the trend is reversed, and cross-sectional area decreases downstream from a value of 25,000 m^2 at RK 800 to 16,500 m^2 near HOP (Fig. 7A). Interestingly, the relative change in cross-sectional area from low- to high-water discharge varies spatially (Fig. 7B): Above RK 400, cross-sectional area increases threefold, and below RK 400, the change in cross-sectional area decreases, approaching unity below RK 200. During low-water discharge, minor undulations in channel cross-sectional area occur between RK 400 and 600, associated with regional increase in channel-bed elevation (e.g., Harmar and Clifford, 2007); however, these undulations do not affect the overall trend of increasing cross-sectional area downstream and are therefore not discussed in further detail.

Changes to cross-sectional area arise due to adjustments in flow depth and width in the lower Mississippi River. Upstream of backwater influence (i.e., >RK 650), the increase in river stage from low- to high-water discharge roughly doubles flow depth (i.e., 100% increase in flow

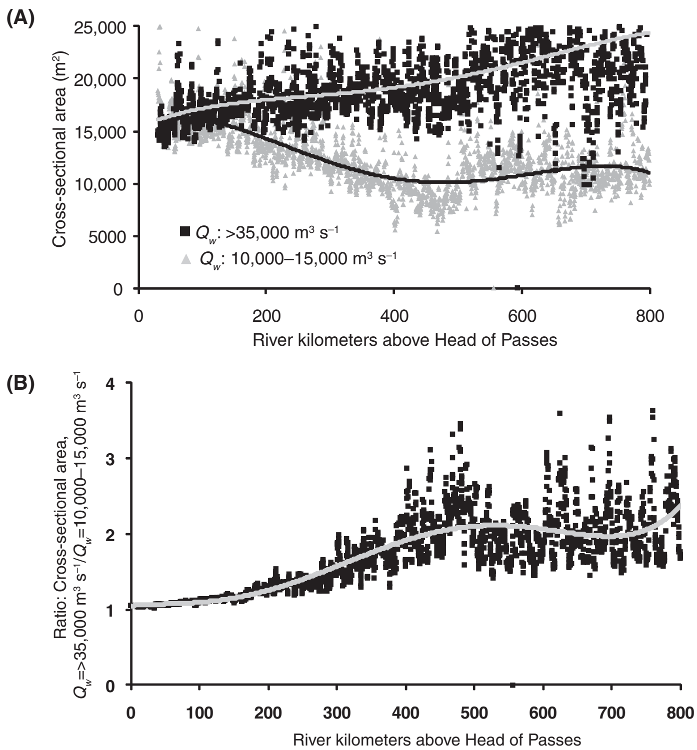

Figure 7. (A) Cross-sectional area of flow for the lower 800 km of the Mississippi River, calculated at each transect for two water discharges (low and high, respectively): 10,000–15,000 $m^3 s^{-1}$ and >35,000 $m^3 s^{-1}$. Regression functions are fit to the values to illustrate a smoothed trend. Note that cross-sectional area of flow increases downstream during low-water discharge; this trend is reversed during high-water discharge, when flow area decreases downstream. (B) Ratio of cross-sectional flow areas, calculated from the cross-sectional area measurements. The variability for cross-sectional area is relatively large upstream of RK 400 (2–3×), and, downstream of RK 200, it converges to unity.

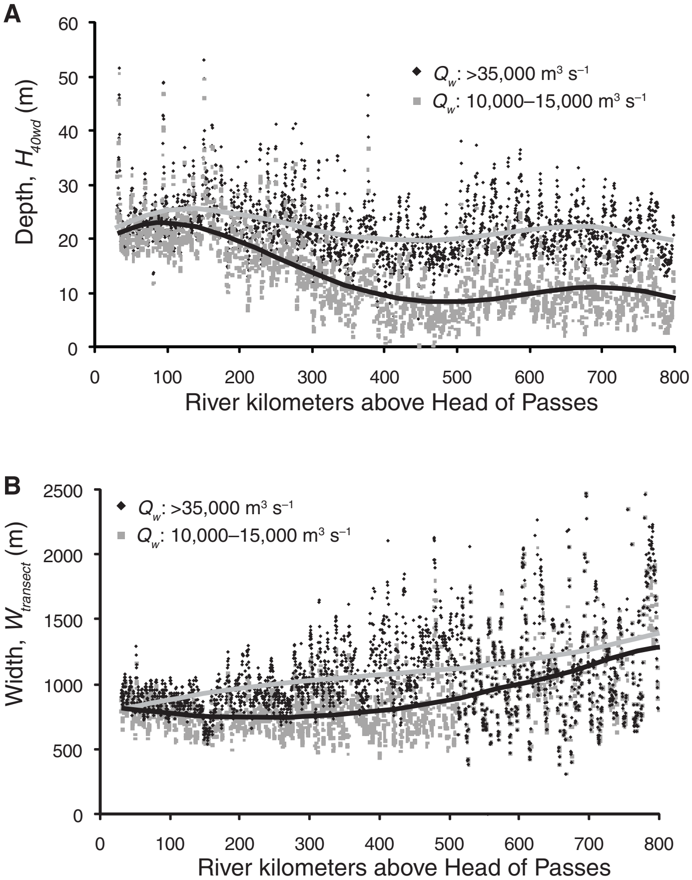

Figure 8. (A) Flow depth (H_{40wd}), measured for each transect for water discharges 10,000–15,000 m^3 s^{-1} and >35,000 m^3 s^{-1}. H_{40wd} was determined for each transect by calculating the difference between the water-surface elevation for the respective water discharge, and the fortieth percentile elevation for each channel transect (η_{40}). (B) Transect width ($w_{transect}$) was measured for water discharges 10,000–15,000 m^3 s^{-1} and >35,000 m^3 s^{-1}. Regressions are fit to the data to illustrate the downstream trends (gray regression fit to >35,000 m^3 s^{-1} data, and black regression fit to 10,000–15,000 m^3 s^{-1} data).

depth; Fig. 8A). However, progressing downstream through the backwater segment of the river, the increase in flow depth from low- to high-water discharge is increasingly minor, so that downstream of RK 150, flow depth only increases ~10% from low- to high-water discharge (Figs. 3 and 8A). Width also varies as a function of water discharge, with the magnitude decreasing downstream through the backwater reach (Fig. 8B).

Calculated Water Velocity in the Lower Mississippi River

Given conservation of water discharge, variations in calculated water-flow velocity arise due to changes in cross-sectional area. Figure 9A plots transect velocity values calculated for water-discharge conditions measuring 11,750 m^3 s^{-1} and 38,400 m^3 s^{-1} (water discharges when shear velocity and sediment transport have been measured), determined for the water-discharge bins of 10,000–15,000 and >35,000 m^3 s^{-1}, respectively. Six-order polynomial regression functions were fit to the data to illustrate the velocity trend for these cases. Figure 9B plots only the six-order polynomial regression functions for four additional discharge cases: low- (Q_w = 7500 m^3 s^{-1}), moderate- (Q_w = 17,500 and 22,500 m^3 s^{-1}), and high-water discharge (Q_w = 40,000 m^3 s^{-1}), using $A_{transect}$ values determined for water discharge bins 5000–10,000 m^3 s^{-1}, 15,000–20,000 m^3 s^{-1}, 20,000–25,000 m^3 s^{-1}, and >35,000 m^3 s^{-1}. These values were compared to velocity data reported by the USACE (mean velocity at 60% of the local flow depth, which approximates the depth-averaged velocity) at three locations in the lower river (http://www.mvn.usace.army.mil/eng/edhd/watercon.htm): Tarbert Landing (RK 493), Baton Rouge (RK 367), and New Orleans (RK 165). The range bars fit to the model values at each of these three sites represent the range of high- and low-water velocities calculated within 5 km upstream and downstream of the survey site, and these range bars contain the measured data. The gray shadowing in Figure 9B represents the regression values ± one standard deviation of all transect velocity values determined in a 15 km window, which is sufficient to cover a typical bend and straight-reach segment in the Mississippi River.

For a constant water discharge, there is nonuniform flow in the lower Mississippi River (Fig. 9B); for example, during low-water discharge (7500 m^3 s^{-1}), there is a distinct deceleration of water-flow velocity in the Mississippi River starting at RK 550 (1.07 m s^{-1}) and extending to HOP (0.49 m s^{-1}), and during high-water discharge (40,000 m^3 s^{-1}), there is flow acceleration from RK 350 to HOP (2.14–2.44 m s^{-1}). Furthermore, the increase in water velocity from low- to high-water discharge is not spatially consistent (Fig. 9): Water velocity increases by less than a factor of 2 upstream of RK 400 (~1.3 m s^{-1} to ~2.1 m s^{-1}), but downstream of RK 200, water velocity increases by a factor of 3 (~0.7 m s^{-1} to ~2.3 m s^{-1}).

Sediment Transport and Channel-Bed Elevation Changes in the Lower Mississippi River

Dimensional bed-load transport rates for all transects, determined for low- and high-water discharges, are presented in Figure 10A; the smoothed transport values were computed using the regression functions fit to the water-velocity data (i.e., regression functions in Fig. 9A). The range bars on Figure 10A near RK 40 represent measured bed-form transport rates during the respective water-discharge conditions (Nittrouer et al., 2011a). Bed-load transport computed for four water-discharge ranges is shown in Figure 10B: low- (Q_w = 7500 m^3 s^{-1}), moderate- (Q_w = 17,500 and 22,500 m^3 s^{-1}), and high-water discharge (Q_w = 40,000 m^3 s^{-1}). These transport values were calculated using the velocity values provided by the regression functions shown in Figure 9B.

Modeled bed-load sediment transport in the Mississippi River is spatially and temporally variable. The smoothed transport values presented in Figure 10A show that bed-load sediment transport increases fortyfold at RK 40 from low- to high-water discharge (2.1×10^{-5} to 8.4×10^{-4} m^2 s^{-1}); additionally, these values

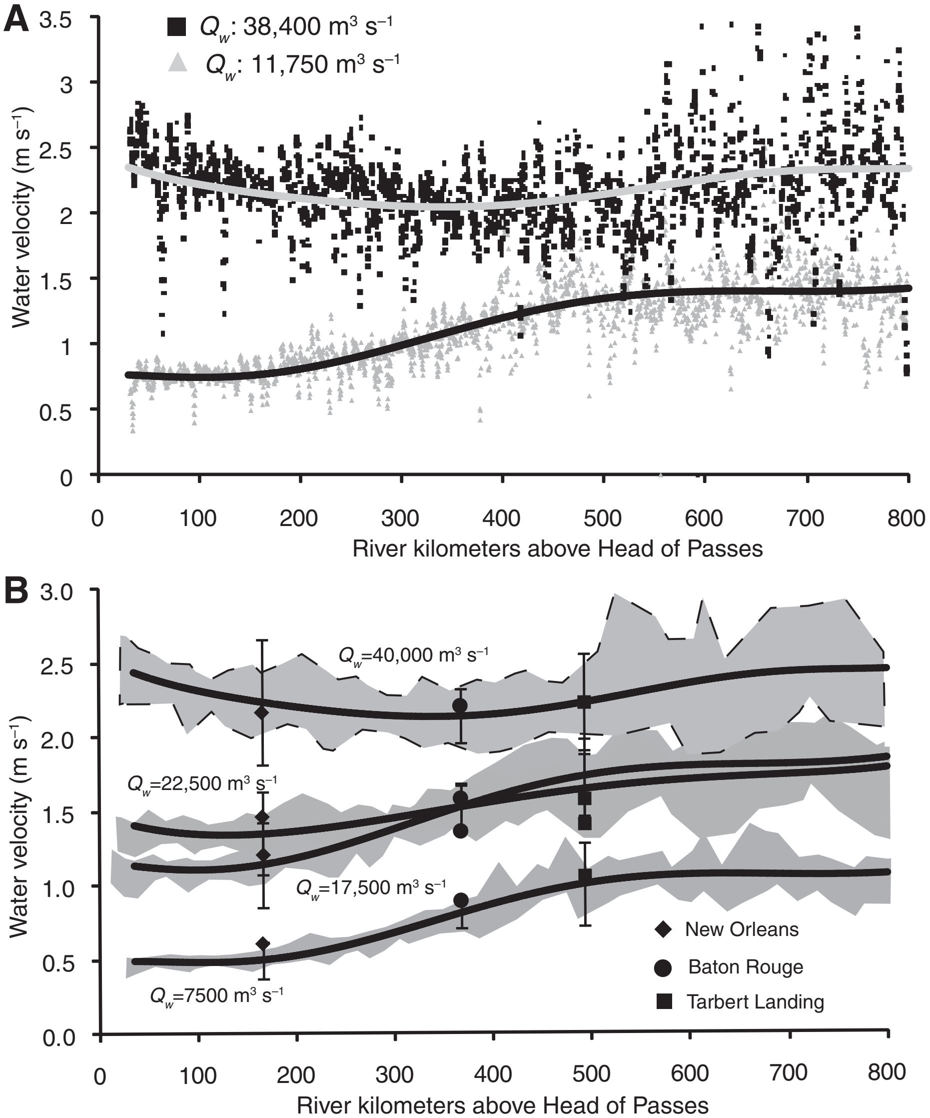

Figure 9. (A) Water velocity values calculated for a low-water discharge, 11,750 m^3 s^{-1}, and a high-water discharge, 38,400 m^3 s^{-1}. Velocity was determined at each transect by dividing the water discharge by cross-sectional area, determined in this figure for discharge ranges 10,000–15,000 m^3 s^{-1} and >35,000 m^3 s^{-1}. Analyses stop at RK 35, where loss of water from the Mississippi River channel becomes significant. Values are fit with regression functions to illustrate the smoothed trend. These values show a depreciation of water velocity in the backwater segment of the lower Mississippi River (below RK 400) during low-water discharge, and an increase in the backwater segment during high-water discharge. These conditions are associated with the downstream increase in cross-sectional area of flow during low-water discharge, and the downstream decrease in cross-sectional area of flow during high-water discharge (see Fig. 7). (B) Regression functions (black lines) determined for calculated water velocity values given for low- (7500 m^3 s^{-1}), moderate- (17,500 m^3 s^{-1} and 22,500 m^3 s^{-1}), and high-water discharges (40,000 m^3 s^{-1}). The gray shading depicts the ± 1 standard deviation from the calculation, determined by averaging calculated values over 15 km segments of the river (high flow is outlined with a dashed line to distinguish from the moderate-water discharges). Note the spatial variation for calculated flow velocity for various discharge conditions. Regression functions were constrained by water velocity measurements reported by the USACE, collected at Tarbert Landing, Baton Rouge, and New Orleans (mean flow velocity measured at 60% of the local flow depth). Range bars represent the variation of calculated velocity values within 5 km upstream and downstream of the measurement sites, so these range bars contain the measured velocity values.

are corroborated by measured bed-form transport rates. Farther upstream, near RK 500, bed-load sediment flux increases only fourfold over the same discharge range (1.69×10^{-4} to 6.25×10^{-4} m^2 s^{-1}). These values demonstrate a significant spatial and temporal departure for bed-load sediment flux in the lower river below RK 550. Bed-load sediment flux varies spatially and as a function of water discharge (Fig. 10B): During low-water discharge (Q_w = 7500 m^3 s^{-1}), there is a 26-fold decrease in transport between RK 550 (5.69×10^{-5} m^2 s^{-1}) and RK 100 (2.22×10^{-6} m^2 s^{-1}). During a moderate-water discharge (Q_w = 17,500 m^3 s^{-1}), flux decreases downstream by a factor of ~5 (3.57×10^{-4} m^2 s^{-1} at RK 550, and 7.54×10^{-5} m^2 s^{-1} RK 100), and for a water discharge of 22,500 m^3 s^{-1}, flux decreases by a factor of 2 (3.09×10^{-4} at RK 550 and 1.59×10^{-4} m^2 s^{-1} at RK 100). Bed-load transport for high-water discharge (40,000 m^3 s^{-1}) is relatively uniform downstream, until RK 350 (6.23×10^{-4} m^2 s^{-1}), where the flux begins and continues to increase until near the outlet at RK 40 (9.85×10^{-4} m^2 s^{-1}).

The Exner model uses bed-load sediment transport values evaluated from the regression functions fit to the calculated water-velocity values (e.g., regression functions in Fig. 9B used to calculate bed-material transport in Fig. 10B) to provide smoothed q_s values for the model. When calculated for an average annual hydrograph, the Exner model results (Fig. 11) depict a tendency for the channel bed to aggrade between RK 600 and 150, and a tendency for the channel bed to degrade from RK 150 to the outlet. The implications for these results are explored in greater detail next.

DISCUSSION

Changes in Cross-Sectional Area of Flow, Water Velocity, and Sediment Transport in the Lower Mississippi River

An important finding in this study is the downstream reversal in the trend of cross-sectional area of flow from low- to high-water discharge, and the effect this property has on flow velocity and sediment transport through the backwater segment of the Mississippi River. During low-water discharge, cross-sectional area increases downstream, due to the twofold increase in characteristic flow depth (Fig. 8A). This results in an enlargement of cross-sectional area and leads to the downstream reduction in flow velocity, and therefore the reduction in sediment transport between RK 150 and 600. During high-water discharge, the cross-sectional area decreases downstream, because the channel width decreases and the water-surface

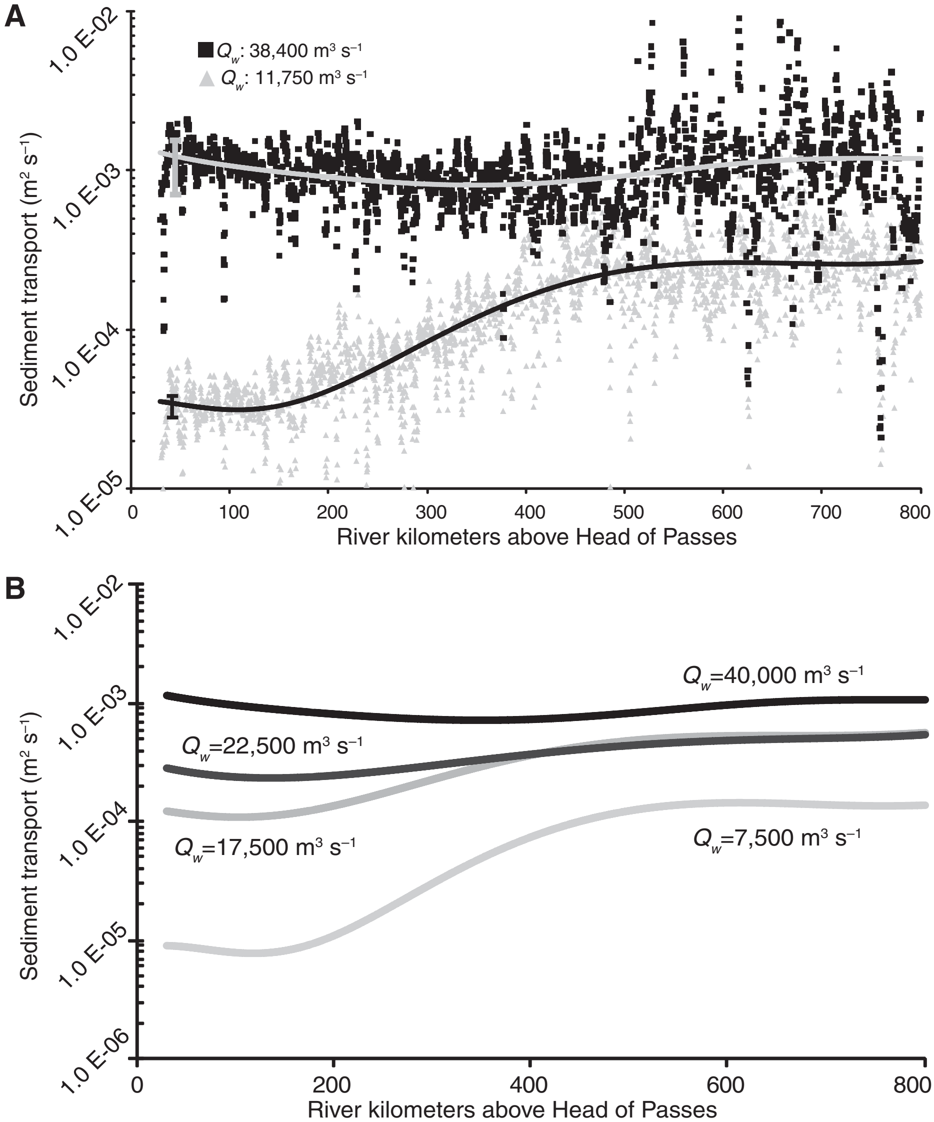

Figure 10. (A) Predicted sediment transport at the location of each channel transect, for the water discharges 11,750 m³ s⁻¹ and 38,400 m³ s⁻¹, using the bed-load formulation of Ashida and Michiue (1972). Range bars near RK 40 show the measured bed-form transport values for the two water-discharge conditions (Nittrouer et al., 2011a). Smooth trends represent sediment flux calculated via regression equations fit to the transect velocity values for the two water-discharge cases (i.e., regressions in Fig. 10). (B) Bed-load sediment transport values predicted for low- (7500 m³ s⁻¹), moderate- (17,500 m³ s⁻¹ and 22,500 m³ s⁻¹), and high-water discharge (40,000 m³ s⁻¹). For this plot, bed-load transport values were calculated based on the regression functions fit to the velocity values predicted for each water-discharge condition (i.e., Fig. 9B). These values show that during low- and moderate-water discharge, bed-load sediment transport decreases significantly in the backwater reach of the Mississippi River. A water discharge near or above 22,500 m³ s⁻¹ provides roughly uniform bed-load flux downstream. During high-water discharge (40,000 m³ s⁻¹), sediment flux increases downstream beginning at ~RK 300.

elevation does not increase commensurately. This leads to the acceleration of water velocity downstream of RK 300, and an increase in sediment transport.

The Exner plot (Fig. 11) was computed based on water-discharge frequency; however, the Mississippi River water discharge in any given year deviates from an average annual hydrograph, and therefore the channel-bed elevation changes computed should not be interpreted as definite yearly aggradation/erosion rates. Instead, these values are meant to serve as a guide for the tendency of the channel bed to aggrade or erode over the lower 800 km of the river, given an average annual hydrograph. The results are nonetheless revealing, because they confirm that the hydrodynamics in the backwater segment of the lower Mississippi River influence aggradation and erosion of the channel bed by driving spatial and temporal divergences in bed-load sediment transport.

There is a propensity for the river to erode its bed below RK 150. This finding is interesting in light of recent work demonstrating that in the final 165 km of the Mississippi River, the channel bed is only partially alluviated, with mobile trains of sandy bed forms and mud deposits (Nittrouer et al., 2011b). In this section of the river, as much as 40% of the channel bed consists of actively eroding, consolidated relict substrate, typically exposed in the channel thalweg. The results of this study show analytically that the lack of alluvial sand cover likely arises due to a downstream increase in sediment transport during high-water discharge that is generated as flow is accelerated in the final 300 km of the river—that is, there is increasing sediment transport capacity downstream for water discharges >23,000 m³ s⁻¹, resulting in the removal of sediment from the bed to the point that the underlying substrate is exposed. It should be kept in mind that erosion of exposed relict substrate cannot be related to the degradation rate calculated via the Exner equation, because this model conserves mass of bed-load sediment flux, calculated at each transect, to determine channel-bed elevation changes (therefore, we treat the exposed substrate as nonerodible).

There is a tendency for the channel bed to aggrade between RK 600 and 150. During low- and moderate-water-discharge conditions, flow velocities decrease through the lower reaches of the Mississippi River due to an increase in channel cross-sectional area, and as a result, bed-load transport decreases downstream, resulting in sediment deposition. Although bed-load transport increases throughout the river during high-water discharge, the spatial increase in transport capacity is not sufficient to remove sediment deposited during low- and moderate-water discharges. Therefore, we hypothesize that the upper reaches of the Mississippi River backwater segment is a region of net sediment storage.

Assessing the Role of Suspended Bed-Material Transport

The focus of this study is on the influence of divergences in bed-load transport on channel-bed elevation; however, a complete assessment of the morphodynamic interactions in the lower

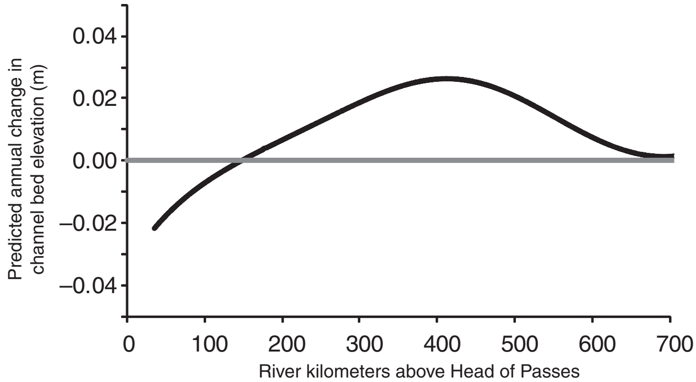

Figure 11. Predicted annual change in channel-bed elevation in the backwater segment of the Mississippi River, using the modeled sediment transport with the Exner equation. The results show that there is a tendency for the channel bed to aggrade between RK 150 and 650 and for the channel bed to erode between Head of Passes (HOP) and RK 150.

Mississippi River should also include predictions for the spatial and temporal changes in the flux of suspended bed materials (i.e., sand). Similar to the nonuniform behavior of bed-load transport, suspended bed-material flux is likely to be spatially and temporally affected by backwater flow conditions. We attempted to assess suspended-sand flux by using a Rouse (1937) profile to predict water-column sand concentration at each transect. The analysis uses predicted skin-friction shear velocity and grain size of the channel-bed sands at each transect. We found that predicted suspended-sand fluxes are extremely sensitive to the input grain sizes. Unfortunately, these sizes are insufficiently resolved from available field data, so that accurate predictions of the time- and space-varying suspended-sand-transport field are not possible. Further field data are needed to constrain the grain-size distribution of sediments, both on the channel bed and in suspension in the lower Mississippi River, before accurate calculations can be made.

While forward modeling of suspended bed-material transport is not possible, there is evidence for a spatially varying sand transport in the Mississippi River backwater reach, based on measurements collected by the U.S. Geological Survey (USGS). Two sampling locations are considered (Fig. 1): St. Francisville (RK 425; USGS station 07373420) and Belle Chasse (RK 120; USGS station 07374525). Data were acquired over two decades (1977–2004) and cover a wide range of water-discharge conditions. Sediment measurements were made primarily using a depth-integrated bag sampler; sand flux was calculated by combining suspended-sand concentration (the portion of the sample with a reported grain size >63 μm) and the respective water discharge during the measurement (Figs. 12A and 12B). Suspended-sand transport is temporally sensitive at both locations: Flux increases more than two orders of magnitude, over an eightfold increase in water discharge (Figs. 12A and 12B).

The interesting aspect of the data is the different sensitivity of suspended-sediment transport to water discharge, as determined using the regression functions fit to both data sets (Fig. 12C). We estimated the minimum water discharge necessary to transport a measurable quantity of sand at both locations by finding the water discharge necessary to produce a detectable volume of sand. This threshold is set at 0.01 m^3 s^{-1} sand transport, which, for their respective water discharges, is equivalent to ~2–4 mg L^{-1}. Based on this standard, sand flux initiates at St. Francisville when water discharge exceeds 6000 m^3 s^{-1}, and at Belle Chasse when water discharge exceeds 10,000 m^3 s^{-1}. The regression equations show that sand flux is greater at St. Francisville than Belle Chasse until a water discharge of 23,000 m^3 s^{-1}, when sand flux equilibrates at both locations (Fig. 12C). The implication is that suspended-sand transport in the Mississippi River is shut down as far upstream as St. Francisville when water discharge is less than 6000 m^3 s^{-1}. When water discharge exceeds 6000 m^3 s^{-1}, suspended-sand flux is larger at St. Francisville than Belle Chasse. Only when water discharge exceeds 23,000 m^3 s^{-1} does sand flux approach the same value at both sites; however, for water discharges >23,000 m^3 s^{-1}, sand flux is slightly greater at Belle Chasse than St. Francisville. Coincidently, ~23,000 m^3 s^{-1} is also the water discharge threshold when water velocity (Fig. 9) and bed-load sediment transport modeled in this study roughly equilibrate throughout the lower river (Fig. 10).

Figure 12. (A) (*on following page*) Suspended-sand flux at St. Francisville, Louisiana (RK 425) versus Mississippi River water discharge (*n* = 307). Data were compiled from suspended-sediment samples collected by the U.S. Geological Survey from 1978 to 2004 (station 07373420). A regression was fit to the data. A zero sand flux was set at 0.01 m^3 s^{-1} (equivalent to 4 mg L^{-1}; excludes 7% of the data shown). The water discharge for this zero sand flux is 6000 m^3 s^{-1}. Therefore, for water discharge less than this value, suspended-sand flux at St. Francisville is considered zero. (B) Suspended-sand flux at Belle Chasse (RK 120) versus Mississippi River water discharge (*n* = 143). Data were compiled from suspended-sediment samples collected by the U. S. Geological Survey from 1977 to 1997 (station 07374525). A regression was fit to the data, and zero sand flux was set at 0.01 m^3 s^{-1} (equivalent concentration: 2 mg L^{-1}; excludes 20% of the data shown). The water discharge for zero sand flux is 10,000 m^3 s^{-1}. The threshold discharge is larger than at St. Francisville, indicating that a larger water discharge is necessary to suspend sand at Belle Chasse. We hypothesize that the difference in threshold discharges can be attributed to downstream deceleration of water velocity and reduction in sediment-transport stress during low- and moderate-water discharge, similar to the bed-load transport model results discussed in this study. (C) Comparison of regression functions fit to the suspended-sand data from St. Francisville and Belle Chasse. The regression functions indicate that for a water discharge less than 6000 m^3 s^{-1}, sand flux is negligible for the lower 425 km of the Mississippi River; for a water discharge of 6000–23,000 m^3 s^{-1}, sand transport is greater at St. Francisville. A water discharge of 23,000 m^3 s^{-1} equilibrates suspended-sand flux between the two sites; for water discharges greater than this value, sand flux is slightly greater at Belle Chasse than St. Francisville. Average yearly suspended-sand flux was calculated using average annual water discharge and the formulas for the regression functions fit to both data sets. The analysis depicts 20% larger sand flux at St. Francisville than Belle Chasse, and therefore we hypothesize that sand is stored in the channel between the two locations.

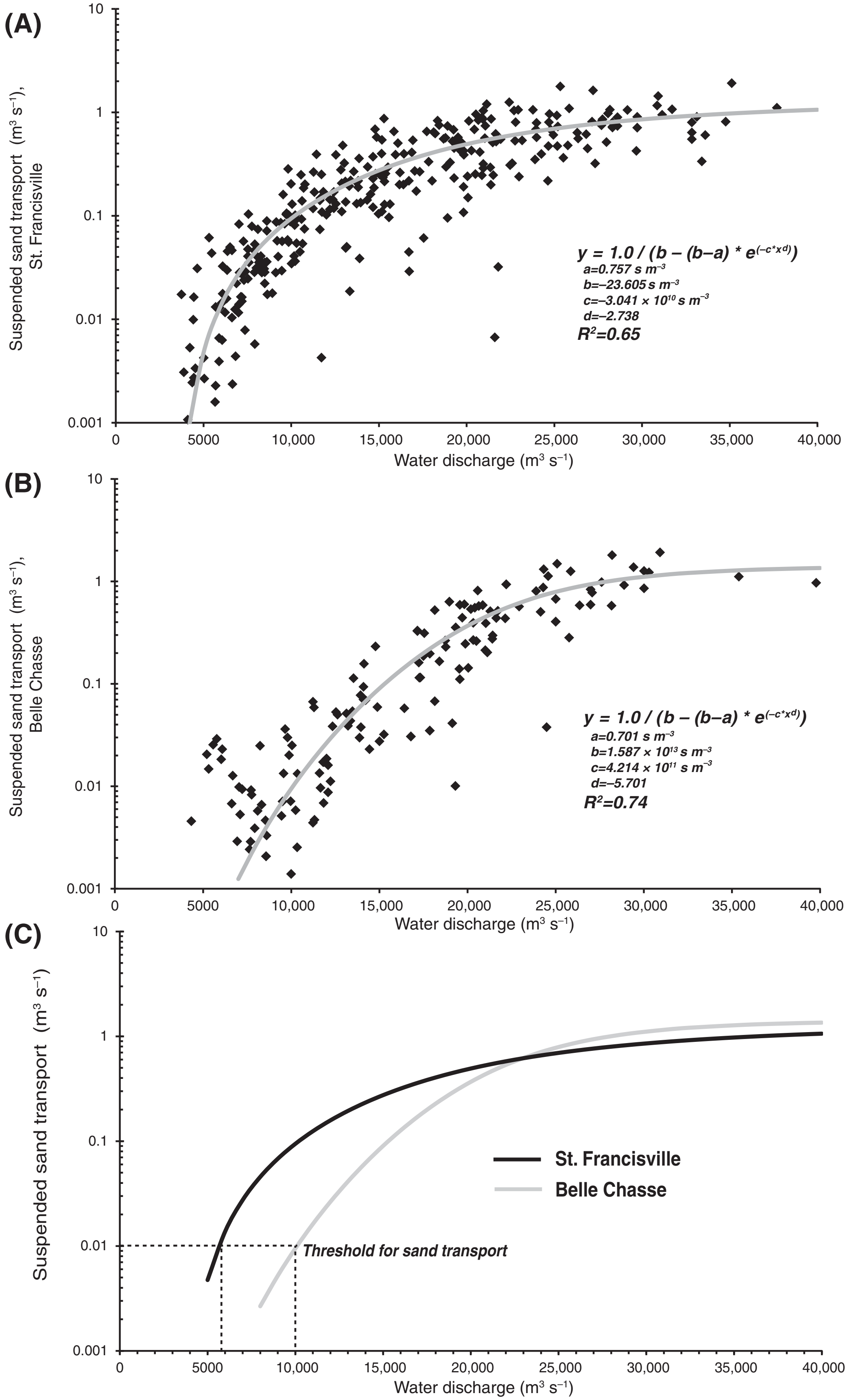

(A)
Suspended sand transport (m3 s−1), St. Francisville
Water discharge (m3 s−1)
y = 1.0 / (b – (b–a) * e(–c*xd))
a=0.757 s m−3
b=–23.605 s m−3
c=–3.041 × 10^10 s m−3
d=–2.738
R2=0.65
(B)
Suspended sand transport (m3 s−1), Belle Chasse
Water discharge (m3 s−1)
y = 1.0 / (b – (b–a) * e(–c*xd))
a=0.701 s m−3
b=1.587 × 10^13 s m−3
c=4.214 × 10^11 s m−3
d=–5.701
R2=0.74
(C)
Suspended sand transport (m3 s−1)
Water discharge (m3 s−1)
St. Francisville
Belle Chasse
Threshold for sand transport
0.001
0.01
0.1
1
10
0
5000
10,000
15,000
20,000
25,000
30,000
35,000
40,000

Figure 12.

Sand transport measured at St. Francisville and Belle Chasse follow a similar trend to predicted bed-load movement: greater flux upstream during low- and moderate-water discharge (<23,000 m^3 s^{-1}), and slightly greater flux farther downstream during high-water discharge (>23,000 m^3 s^{-1}). While there is scatter in the suspended-sand data, it is notable that the best-fit regression functions are independently consistent with the spatial and temporal trends predicted by bed-load transport modeling presented in this study. As such, we hypothesize that spatially varying flow conditions in the backwater segment of the Mississippi River also influence suspended-sand flux.

The regression functions fit to the suspended-sand data were used to evaluate the impact of backwater hydrodynamic conditions on mass flux of suspended sand at both locations over an average annual hydrograph. Daily water-discharge measurements from Tarbert Landing were collected over the period 1961–2008; the data were binned at 250 m^3 s^{-1} increments, and the frequency of occurrence was determined for each bin. The average water discharge for the bin was then inserted into both regression functions, and the output was multiplied by the frequency of occurrence. Sand volume was then summed for all bins and totaled for a 1 yr period. Total yearly suspended-sand flux calculated at St. Francisville (8.65×10^6 m^3 yr^{-1}; 22.9×10^6 T yr^{-1}) is ~20% larger than yearly suspended-sand flux at Belle Chasse (7.17×10^6 m^3 yr^{-1}; 19.0×10^6 T yr^{-1}). This disparity indicates the possibility that suspended sand is stored between the two monitoring stations. Furthermore, the imbalance in suspended-sand transport may produce channel-bed aggradation, in addition to that estimated based on the spatial divergence in bed-load flux evaluated in this study (Fig. 11).

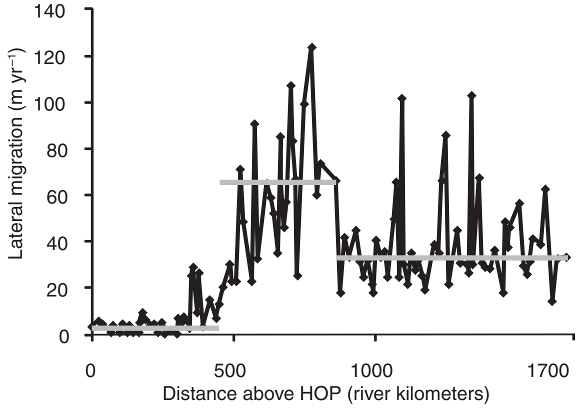

Figure 13. Lateral migration for the lower Mississippi River, from Cairo, Illinois (RK 1700) to Head of Passes (HOP). Data were reported by Hudson and Kesel (2000). Upstream of RK 800, average lateral migration is ~38 m yr^{-1}. Between RK 400 and 800, where the Mississippi River transitions to backwater flow, lateral migration increases to ~62 m yr^{-1}. Downstream of RK 300, the river transitions to a mixed bedrock-alluvial channel (Nittrouer et al., 2011b), and lateral migration diminishes significantly. These changes in the rates of lateral mobility coincide with the regions of predicted channel-bed aggradation and erosion.

Spatially Varying Sediment Transport: Implications for Channel Planform and Kinematics

In the lower 1700 km of the Mississippi River, lateral migration rates have been measured by Hudson and Kesel (2000). Their data show that lateral migration is relatively consistent above RK 700 (~38 m yr^{-1}), and increases between RK 450 and 700 (~62 m yr^{-1}) before essentially stopping for the segment of river downstream of RK 300 km (<1 m yr^{-1}; Fig. 13). Theoretical models indicate that the transport of bed-material sediment is a driver for lateral mobility, because the movement of sediment to the downstream end of channel bars redirects the thalweg to the opposite bank, leading to bank erosion and widening of the river channel; uniform channel width is maintained by commensurate sediment accumulation on the interior bar (Ikeda et al., 1981; Nelson and Smith, 1989b; Hasegawa, 1989).

Channel-bar development in the Mississippi River is likely influenced by spatial divergences in sediment transport, and therefore a relationship may arise between rates of lateral migration (measured by Hudson and Kesel, 2000) and regions of aggradation and degradation evaluated in this study (Fig. 11). At RK 700, where the Mississippi River migrates laterally at a uniform rate, the Exner model shows spatially equilibrated sediment transport and therefore little tendency for aggradation or erosion of the channel bed. Interestingly, the increase in the rate of channel mobility for RK 400–800 coincides with the location of predicted channel-bed sediment aggradation (Fig. 11). Downstream of RK 300, lateral migration nearly ceases in the region where the channel bed tends to erode. Therefore, at minimum, the spatial trends for lateral mobility coincide with predicted trends for aggradation and erosion of channel-bed sediments. However, a stronger morphodynamic link likely exists among spatially divergent sediment flux, the evolution of channel bars, and rates of channel migration.

The channel-bed morphology and kinematics of the lower Mississippi River are similar to those described for the Teshio River (Ikeda, 1989), and the changing fluvial characteristics of the Teshio River also coincide with the system's backwater length. For example, both rivers display a change in channel-bed character and migration rates as they approach their outlets. Downstream of their respective backwater lengths, both systems have diminished lateral migration associated with channel incision into consolidated paleodeltaic sediments and limited alluvial cover of the channel bed; both channels are relatively fixed due to incision into floodplain deposits. Ikeda (1989) showed that the composition of the Teshio River's channel bed coarsens near the backwater transition, and that this coincides with increased lateral migration of the channel. Similar channel morphology and kinematics exist for both river systems, scaled by their respective backwater lengths, and the work here shows that these changes likely arise due to spatial divergences in the bed-material sediment transport associated nonuniform water-flow conditions.

Finally, there may also be an important link between flow dynamics in the Mississippi River and the location of the first distributary channel, the Atchafalaya River (RK 505; Fig. 1). A requisite for fluvial avulsion is the positioning of the river's water surface above the surrounding floodplain (Heller and Paola, 1996; Bryant et al., 1995; Mohrig et al., 2000). This condition is present at RK 505, and it is likely augmented through time by deposition of sediments to the channel bed as predicted in this study, particularly if aggradation is considered over the time scale of the modern Mississippi River channel (~1000 yr). The backwater length scale ($L_b = HS^{-1}$) has been related to the occurrence of the first distributary node in a number of other lowland river systems nearing the coastline (Jerolmack, 2009; Jerolmack and Swenson, 2007). This study confirms that changing hydrodynamic conditions in the backwater segment of rivers generate sediment deposition in the channel, and therefore play an important role in facilitating channel avulsions that lead to formation of fluvial distributary channels.

CONCLUSIONS

The principal contribution of this study is to demonstrate that the flux of bed materials is significantly modified through the backwater reach of the Mississippi River. The spatial and temporal divergence in sediment transport results in a tendency for the channel bed to aggrade in the upper segment and degrade in the lower segment of the backwater reach. At minimum, these changing channel properties coincide with dynamic rates of lateral mobility, and likely influence the positioning of a modern distributary node. However, we propose a morphodynamic link, whereby changing hydrodynamics in the backwater reach affect sediment transport, which in turn influences channel morphology and kinematics. The interaction of the processes is the focus of ongoing research. Here, we summarize the primary findings discussed in this study.

Channel cross-sectional data over the normal-flow to backwater transition in the Mississippi River show two distinct trends: (1) During low- and moderate-water discharge, there is a downstream increase in the cross-sectional area flow, and (2) during high-water discharge, cross-sectional flow area decreases downstream. Changing flow area affects calculations for depth-averaged velocity: During low- and moderate-water discharge, flow velocity decreases downstream, and during high-water discharge, water-flow velocity increases downstream.

Bed-load transport rates, modeled using calculated flow velocity converted to skin-friction shear stress, vary spatially and also as a function of water discharge through the backwater segment of the Mississippi River. During low- and moderate-water discharge, there is a downstream decrease in bed-material transport, and during high-water discharge, there is a downstream increase in bed-material transport. The predicted rates of sediment transport were coupled with an Exner model run for an average yearly hydrograph and used to evaluate a tendency for the channel bed to aggrade in the upper segment of the backwater reach (RK 600–150), and a tendency for channel bed to erode near the river outlet (downstream of RK 150).

A spatial imbalance for suspended-sand transport in the lower Mississippi River is noted, and the patterns are similar to bed-load transport. The data show that sand flux is rarely equilibrated between the St. Francisville and Belle Chasse: For low- and moderate-water discharge, measureable suspended-sand flux is larger at St. Francisville, and for high-water discharge, suspended-sand flux is slightly greater at Belle Chasse. When considered over an average annual hydrograph, total sand volume transported is roughly 20% greater at St. Francisville, and this imbalance points to the possibility of additional net storage of sand within the lower reaches of the Mississippi River in addition to bed-load transport disequilibrium predicted in this study.

Several dynamic planform characteristics of the Mississippi River coincide with the predicted locations of deposition and erosion of the channel bed. Aggradation of the channel bed, in the upper reaches of the backwater segment, arises where high rates of lateral migration are measured. Deposition of bed-load sediment contributes to the growth of channel bars, and therefore enhances lateral migration. Conversely, near the fluvial outlet, channel-bed erosion limits bar growth and lateral mobility. Furthermore, the location of the modern avulsion node for the Mississippi River coincides with the region of predicted sediment aggradation. The deposition of sediment in the river channel will facilitate avulsions and lead to the development distributary channels. We postulate that channel-bed aggradation at the normal-flow to backwater transition has located the modern Atchafalaya distributary channel.

Backwater hydrodynamics associated with a river nearing the coastline will operate in all lowland river systems, and should be especially pronounced in deep and/or low-sloping rivers, where nonuniform flow can extend tens to hundreds of kilometers above the outlet. Therefore, similar dynamic channel properties are likely to arise in past and present lowland river systems, and ultimately this hydrodynamic influence will affect channel morphology and the character and timing of sediment transferred from rivers to marine settings.

ACKNOWLEDGMENTS

This study was facilitated by the field-survey data of the Mississippi River channel collected by the United States Army Corps of Engineers and provided by O. Harmar. We thank Gary Parker for providing insight and review of this study. We also thank two anonymous referees for their reviews and input. This research was supported by the National Science Foundation, via the National Center for Earth-surface Dynamics under agreement EAR-0120914. This work was also supported by National Science Foundation grant EAR0948224 to J.A.N., and by the ACS Petroleum Research Fund grant to M.P.L.

REFERENCES CITED

Allison, M.A., and Meselhe, E.A., 2010, The use of large water and sediment diversions in the lower Mississippi River (Louisiana) for coastal restoration: Journal of Hydrology (Amsterdam), v. 387, p. 346–360, doi:10.1016/j.jhydrol.2010.04.001.

Ashida, K., and Michiue, M., 1972, Study of hydraulic resistance and bed-load transport rate in alluvial streams: Transactions of the Japan Society of Civil Engineering, v. 1972, p. 59–69, doi:10.2208/jscej1969.1972.206_59.

Bryant, M., Falk, P., and Paola, C., 1995, Experimental study of avulsion frequency and rate of deposition: Geology, v. 23, p. 365–368, doi:10.1130/0091-7613(1995)023<0365:ESOAFA>2.3.CO;2.

Chaudhry, M.H., 2008, Open-Channel Flow: New York, Springer, 523 p.

Chow, V.T., 1959, Open-Channel Hydraulics: New York, McGraw-Hill, 680 p.

Harmar, O.P., 2004, Morphological and Process Dynamics of the Lower Mississippi River [Ph.D. dissertation]: Nottingham, UK, The University of Nottingham, 430 p.

Harmar, O.P., and Clifford, N.J., 2007, Geomorphological explanation of the long profile of the lower Mississippi River: Geomorphology, v. 84, p. 222–240, doi:10.1016/j.geomorph.2006.01.045.

Hasegawa, K., 1989, Studies on qualitative and quantitative prediction of meander channel shift, *in* Ikeda, S., and Parker, G., eds., River Meandering: London, Washington, D.C., American Geophysical Union, p. 215–236.

Heller, P.L., and Paola, C., 1996, Downstream changes in alluvial architecture: An exploration of controls on channel-stacking patterns: Journal of Sedimentary Research, v. 66, p. 297–306.

Hudson, P.F., and Kesel, R.H., 2000, Channel migration and meander-bend curvature in the lower Mississippi River prior to major human modification: Geology, v. 28, p. 531–534, doi:10.1130/0091-7613(2000)28<531:CMAMCI>2.0.CO;2.

Ikeda, H., 1989, Sedimentary controls on channel migration and origin of point bars in sand-bedded meandering rivers, *in* Ikeda, S., and Parker, G., eds., River Meandering: London, Washington, D.C., American Geophysical Union, p. 51–68.

Ikeda, S., Parker, G., and Sawai, K., 1981, Bend theory of river meanders: Part 1. Linear development: Journal of Fluid Mechanics, v. 112, p. 363–377, doi:10.1017/S0022112081000451.

Jerolmack, D.J., 2009, Conceptual framework for assessing the response of delta channel networks to Holocene sea level rise: Quaternary Science Reviews, v. 28, p. 1786–1800, doi:10.1016/j.quascirev.2009.02.015.

Jerolmack, D.J., and Swenson, J.B., 2007, Scaling relationships and evolution of distributary networks on wave-influenced deltas: Geophysical Research Letters, v. 34, p. L23402, doi:10.1029/2007GL031823.

Lane, E.W., 1957, A Study of the Shape of Channels Formed by Natural Streams Flowing in Erodible Material: Missouri River Division Sediment Series Report 9: Omaha, Nebraska, U.S. Army Corps of Engineers, p. 1–106.

Mohrig, D., Heller, P.L., Paola, C., and Lyons, W.J., 2000, Interpreting avulsion processes from ancient alluvial sequences: Guadalope-Matarranya system (northern Spain) and Wasatch Formation (western Colorado): Geological Society of America Bulletin, v. 112, p. 1787–1803, doi:10.1130/0016-7606(2000)112<1787:IAPFAA>2.0.CO;2.

Nelson, J.M., and Smith, J.D., 1989a, Flow in meandering channels with natural topography, *in* Ikeda, S., and Parker, G., eds., River Meandering: London, Washington, D.C., American Geophysical Union, p. 69–102.

Nelson, J.M., and Smith, J.D., 1989b, Evolution and stability of erodible channel beds, *in* Ikeda, S., and Parker, G., eds., River Meandering: London, Washington, D.C., American Geophysical Union, p. 321–377.

Nittrouer, J.A., Allison, M.A., and Campanella, R.C., 2008, Bedform transport rates for the lowermost Mississippi River: Journal of Geophysical Research, v. 113, doi:10.1029/2007JF000795.

Nittrouer, J.A., Mohrig, D., and Allison, M.A., 2011a, Punctuated transport of bed materials in the lowermost Mississippi River: Journal of Geophysical Research-Earth Surface, doi:10.1029/2011JF002026 (in press; available via AGU Papers in Press).

Nittrouer, J.A., Mohrig, D., and Allison, M.A., 2011b, The lowermost Mississippi River: A mixed bedrock-alluvial channel: Sedimentology, doi:10.1111/j.1365-3091.2011.01245.x (in press).

Paola, C., and Mohrig, D., 1996, Paleohydraulics revisited: Paleoslope estimation in coarse-grained braided rivers: Basin Research, v. 8, p. 243–254, doi:10.1046/j.1365-2117.1996.00253.x.

Paola, C., and Voller, V.R., 2005, A generalized Exner equation for sediment mass balance: Journal of Geophysical Research, v. 110, F04014, doi:10.1029/2004JF000274.

Parker, G., 2004, 1D Sediment Transport Morphodynamics with Applications to Rivers and Turbidity Currents: E-book, Minneapolis, St. Anthony Falls Laboratory, University of Minnesota, http://vtchl.uiuc.edu/people/parkerg/morphodynamics_e-book.htm; accessed 5 August 2010.

Parker, G., Muto, T., Akamatsu, Y., Dietrich, W.E., and Lauer, J.W., 2008, Unravelling the conundrum of river response to rising sea-level from laboratory to field: Part II. The Fly-Strickland River system, Papua New Guinea: Sedimentology, v. 55, p. 1657–1686, doi:10.1111/j.1365-3091.2008.00962.x.

Rouse, H., 1937, Modern conceptions of the mechanics of fluid turbulence: Transactions of the American Society of Civil Engineers, v. 102, p. 463.

Shields, A., 1936, Application of similarity principles and turbulence research to bed-load movement: Miteilungen der Preussischen Versuchsanstalt für Wasserbau und Schiffbau, Berlin (translated to English by W.P. Ott and J.C. van Uchelen): Pasadena, California, California Institute of Technology Hydraulics Laboratory, 36 p.

Snyder, N.P., Wright, S.A., Alpers, C.N., Flint, L.E., Holmes, C.W., and Rubin, D.M., 2006, Reconstructing depositional processes and history from reservoir stratigraphy: Englebright Lake, Yuba River, northern California: Journal of Geophysical Research, v. 111, p. F04003, doi:10.1029/2005JF000451.

U.S. Army Corps of Engineers (USACE), 1935, Studies of River Bed Materials and their Movement, with Special Reference to the Lower Mississippi River: Vicksburg, Mississippi, U.S. Waterways Experiment Station Paper 17, 161 p.

Science Editor: Christian Koeberl
Associate Editor: Joan Florsheim

Manuscript Received 23 February 2011
Revised Manuscript Received 13 July 2011
Manuscript Accepted 20 July 2011

Printed in the USA